Applied Physics Letters

RESEARCH ARTICLE | JANUARY 18 1999

Structural properties and Raman modes of zinc blende InN epitaxial layers

A. Tabata; A. P. Lima; L. K. Teles; L. M. R. Scolfaro; J. R. Leite; V. Lemos; B. Schöttker; T. Frey; D. Schikora; K. Lischka

Check for updates

Appl. Phys. Lett. 74, 362–364 (1999)
https://doi.org/10.1063/1.123072

View Online
Export Citation

Articles You May Be Interested In

Raman phonon modes of zinc blende In x Ga 1−x N alloy epitaxial layers

Appl. Phys. Lett. (August 1999)

Deposition factors and band gap of zinc-blende AlN

J. Appl. Phys. (March 2001)

Raman study of collective plasmon-longitudinal optical phonon excitations in cubic GaN and Al x Ga 1−x N epitaxial layers

J. Appl. Phys. (May 2002)

06 November 2025 18:57:40

Webinar From Noise to Knowledge
May 13th – Register now
Zurich Instruments
Universität Konstanz

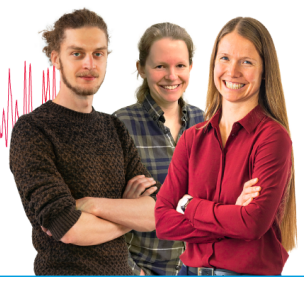

AIP Publishing

Structural properties and Raman modes of zinc blende InN epitaxial layers

A. Tabata, A. P. Lima, L. K. Teles, L. M. R. Scolfaro, and J. R. Leite
Universidade de São Paulo, Instituto de Física, Caixa Postal 66318, 05315-970 São Paulo, SP, Brazil

V. Lemos
Instituto de Física Gleb Wataghin, Universidade Estadual de Campinas, 13083-970 Campinas, SP, Brazil

B. Schöttker,[a] T. Frey, D. Schikora, and K. Lischka
Universität/GH Paderborn, FB 6 Physik, Warburger Str. 100, 33098 Paderborn, Germany

(Received 9 July 1998; accepted for publication 8 November 1998)

We report on x-ray diffraction and micro-Raman scattering studies on zinc blende InN epitaxial films. The samples were grown by molecular beam epitaxy on GaAs(001) substrates using a InAs layer as a buffer. The transverse-optical (TO) and longitudinal-optical phonon frequencies at Γ of *c*-InN are determined and compared to the corresponding values for *c*-GaN. *Ab initio* self-consistent calculations are carried out for the *c*-InN and *c*-GaN lattice parameters and TO phonon frequencies. A good agreement between theory and experiment is found. © *1999 American Institute of Physics.* [S0003-6951(99)00503-3]

The direct wide band-gap GaN and InN semiconductors in the zinc blende phase are of potential interest for the optoelectronic device technology. Although GaN epitaxial layers have been grown on several cubic substrates,[1] only very few attempts were made to grow zinc blende InN films so far.[2–5] The structural properties of the films, grown on GaAs(001),[2–4] GaP(001),[4] and GaAs(111),[5] substrates were investigated. It has been argued that cubic (*c*-) InN inclusions in the wurtzite InGaN quantum well layer should be the active media in optoelectronic devices emitting in the green ultraviolet (UV) spectral region.[6] Thus, the investigations on the properties of *c*-InN are important for the applications based on both, zinc blende and wurtzite phases of group III-nitride semiconductors.

In this work we report on the molecular beam epitaxial (MBE) growth of zinc blende InN layers and on the investigation of their structural and vibrational properties. The *c*-InN sample was grown on a InAs buffer layer firstly grown on GaAs(001) substrate by plasma-assisted MBE. We have used a Riber 32-system equipped with elemental sources of Ga, As, In, and an Oxford Applied Research CARS25 radio frequency (rf) plasma source for the reactive nitrogen. The growth of the cubic InN material is very unstable with strong tendency to form a polycrystalline or even an amorphous phase, with just a small deviation from the optimized growth conditions. The optimization of our cubic InN sample was done by continuous monitoring the growth process by reflection high energy electron diffraction (RHEED) and a RHEED image recording system. The optimized sample was obtained according to the following procedure: after the growth of the GaAs buffer layer at a temperature of 610 °C, we grew a 300 nm layer of InAs at a temperature of 480 °C under (2×4) reconstruction. The growth of the InN layer was preceded by a nitridation of the InAs surface, which was performed at a reduced temperature of 450 °C, with the As and In sources closed, but with a flux of activated nitrogen on the sample. After the formation of a few monolayers of *c*-InN during the nitridation process, based on the N–As surface anion exchange, the In cell was opened again and we started the growth of *c*-InN at the same temperature (450 °C). From the RHEED pattern, shown in Fig. 1, we can check the pure cubic phase growing on the surface and obtain the lattice constant of *c*-InN. The InN growth rate was 80 nm/h. The thickness of the *c*-InN film was 300 nm.

The crystalline structure of the *c*-InN film was identified by means of x-ray diffraction (XRD) experiments. The measurements were performed on a Philips PW 1710 diffractometer equipped with a standard Cu $K\alpha$ radiation source employing a step size of 0.05° in 2θ. Figure 2 shows the XRD pattern of our InN/InAs/GaAs optimized sample. The diffraction peaks associated to (004) and (002) GaAs planes at $2\theta=66.3°$ and 31.1°, respectively, are clearly seen in the spectrum, as well as the (004) and (002) reflexes of the InAs buffer layer located at $2\theta=61.1°$ and 29.6°, respectively. The cubic phase in the XRD spectrum is identified by the

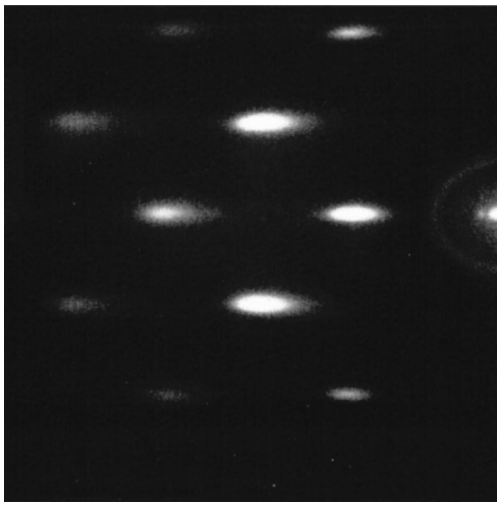

FIG. 1. RHEED pattern taken along the [110] azimuth for the *c*-InN film grown on a InAs buffer film layer on GaAs(001).

[a]Electronic mail: li_bs@physik.uni-paderborn.de

06 November 2025 18:57:40

 © 1999 American Institute of Physics

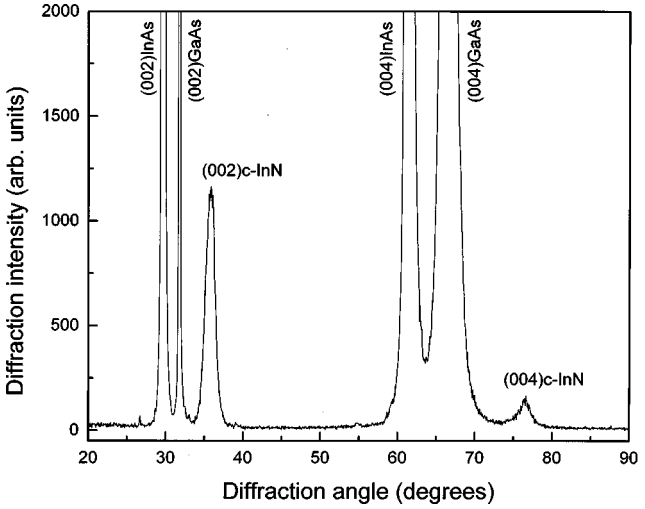

FIG. 2. X-ray diffraction pattern of the *c*-InN film.

presence of peaks at diffraction angles $2\theta = 76.4°$ and 36.1° originating from the zinc blende type InN (004) and (002) planes, respectively. The full width at half maximum of each one of the peaks associated to *c*-InN is about 1.5°. The hexagonal (*h*-) InN, on the XRD spectrum, normally has a peak at $2\theta = 33.0°$ associated to the (0002) plane. However, under the diffraction conditions used here, it could not be resolved because in the hexagonal minority phase the *c* axis is tilted by a few degrees with respect to the cubic majority phase, and in this condition only Bragg peaks originating from the majority phase are possible to be observed.[7]

From our x-ray and RHEED measurements we obtain the *c*-InN lattice constant which is shown in Table I along to the experimental values obtained for *c*-GaN for comparison.[8,9] The result obtained from our experiments is in good agreement with the previous value reported for *c*-InN.[2] In the present work we carried out *ab initio* self-consistent *full potential* linear-augmented-plane-wave (LAPW)[10,11] calculations of the lattice parameters for *c*-InN and *c*-GaN. The theoretical values obtained by us shown in Table I are in good agreement with the experimental results obtained for both semiconductor compounds. They are also in good agreement with the results reported from other calculations.[12–15]

Figure 3 shows room temperature micro-Raman spectra of the InN/InAs/GaAs grown film (a). Figure 3(b) depicts the micro-Raman spectrum of a *c*-GaN sample for comparison. The structural characteristics of this sample are described in Ref. 16 where we report on our previous Raman results for *c*-GaN. In the present work the measurements were carried out at room temperature in backscattering geometry by means of a T6400 Jobin Yvon Raman system. The 514.5 nm

TABLE I. Lattice constants of zinc blende InN and GaN (in Å).

	InN	GaN
Expt.	4.97±0.01[a]; 4.98±0.01[b]	4.50[c], 4.51[d]
Calc.	4.96[a], 5.03[e], 4.79[f], 4.93[g], 4.92[h]	4.55[a], 4.54[e], 4.46[g,h]

[a]This work.
[b]Ref. 2.
[c]Ref. 8.
[d]Ref. 9.
[e]Ref. 12.
[f]Ref. 13.
[g]Ref. 14.
[h]Ref. 15.

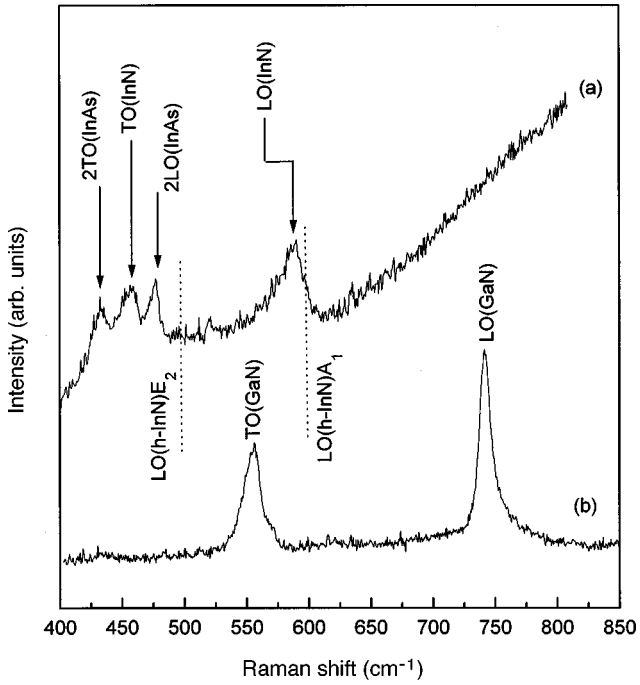

FIG. 3. Room temperature micro-Raman spectra of the *c*-InN sample (a) and of a *c*-GaN sample (b) described in Ref. 16. The two most intense phonon peaks quoted in Ref. 19 for the *h*-InN phase are also indicated.

(2.41 eV) radiation of an argon ion laser was used for excitation. The incident laser beam was unpolarized, and no polarization analyzer was used for the scattered beam. In order to avoid thermal damage, the laser power was kept as low as 50 mW. For zinc blende InN and GaN, the optical phonon modes at the Brillouin zone center belong to the three-dimensional irreducible representation T_2 of the point group T_d. The transverse optical (TO) phonon mode is doubly degenerate while the longitudinal mode (LO) is single degenerate with a higher frequency. In cubic crystal and under backscattering geometry, the longitudinal-optical branch is symmetry allowed, while the transverse-optical branch of the TO mode is forbidden. However, sometimes it becomes allowed due to the existence of a short range perturbation, which brakes the T_d symmetry allowing the detection of the TO mode.

Figure 3(a) shows that for the InN/InAs/GaAs sample, the Raman peaks associated to the *c*-InN as well as to the *c*-InAs phonon modes are clearly resolved. The InAs buffer layer 2TO and 2LO phonon modes are detected at 430 and 479 cm^{-1}, respectively.[17] In order to ascribe the other two peaks clearly seen in Fig. 3(a) to *c*-InN we have to rule out the possibilities that they are arising either from the GaAs buffer layer or from a possible minority hexagonal InN phase. The TO and LO phonon modes of GaAs are at 268.6 and 292.9 cm^{-1}, respectively,[18] thus not seen in Fig. 3(a). On the other hand, recent Raman measurements have shown that the two more intense phonon mode peaks of *h*-InN are at 495 cm^{-1}, ascribed to the E_2 mode, and at 596 cm^{-1} ascribed to the A_1 mode of LO.[19] These values are indicated in Fig. 3. The values 400 (A_1) and 490 cm^{-1} (E_1) for the TO modes of *h*-InN, not shown in Fig. 3, have been reported recently.[20] They are consistent with the expected splitting of our measured T_2 TO frequency in *c*-InN when the symmetry

06 November 2025 18:57:40

TABLE II. Phonon frequencies at Γ for zinc blende InN and GaN (in cm^{-1}).

	InN		GaN	
	TO	LO	TO	LO
Expt.	457	588	555	741
Calc.	453, 540[a]		556, 580[a]	

[a]Ref. 15.

is lowered from T_d to hexagonal.[16] Although there are discrepancies between the reported values for the LO modes in Refs. 19 and 20, the data for *h*-InN indicate that our phonon modes assignments for *c*-InN are correct.

The phonon frequencies at Γ for zinc blende InN and GaN obtained from our Raman data and LAPW calculations are shown in Table II. Recent calculated results obtained by using an *ab initio* linear muffin-tin-orbitals (LMTO) method are included for comparison.[15] No attempts were made by us to compare the experimental results for the *c*-GaN phonon energies with several other calculations available in the literature once the issue here are the *c*-InN properties. The entries in Table II show that a very good agreement is obtained between the experimental results and our LAPW calculations for the *c*-InN and *c*-GaN TO phonon energies. The LMTO calculations somehow overestimate the phonon energy values.

As a consequence of the weaker In–N chemical bond as compared to the Ga–N bond, the lattice parameter of *c*-InN is 10.4% larger than that of *c*-GaN and the phonon modes are displaced to lower energies. In a model where we neglect the bond-bending effects we can infer from the values obtained for the TO energies the ratio between the In–N and Ga–N bond stretchings. We have found that the chemical bond stretching in *c*-InN is about 27% weaker than in *c*-GaN.

This work was performed under partial support of a CAPES/DAAD/PROBAL project within the Brazil/Germany scientific collaboration program. The authors are also indebted to Fapesp and CNPq (Brazilian funding agencies) and VW-Stiftung for partial support.

[1] J. W. Orton and C. T. Foxon, Rep. Prog. Phys. **61**, 1 (1998).
[2] S. Strite, D. Chandrasekhar, D. J. Smith, J. Sariel, H. Chen, N. Teraguchi, and H. Morkoç, J. Cryst. Growth **127**, 204 (1993).
[3] D. Chandrasekhar, D. J. Smith, S. Strite, M. E. Lin, and H. Morkoç, J. Cryst. Growth **152**, 135 (1995).
[4] L. C. Jenkins, T. S. Cheng, C. T. Foxon, S. E. Hooper, J. W. Orton, S. V. Novikov, and V. V. Tret'yakov, J. Vac. Sci. Technol. B **13**, 1585 (1995).
[5] A. Yamamoto, Y. Yamauchi, M. Ohkubo, and A. Hashimoto, J. Cryst. Growth **174**, 641 (1997).
[6] B. A. Weinstein, P. Perlin, N. E. Christensen, I. Gorezyka, V. Iota, T. Suski, P. Wisniewski, M. Osinski, and P. G. Eliseev, Solid State Commun. **106**, 567 (1998).
[7] H. Siegle, L. Eckey, A. Hoffmann, C. Thomsen, B. K. Meyer, D. Schikora, M. Hankel, and K. Lischka, Solid State Commun. **96**, 943 (1995).
[8] T. Lei, T. D. Moustakas, R. J. Graham, Y. He, and S. J. Berkowitz, J. Appl. Phys. **71**, 4933 (1992).
[9] I. Petrov, E. Mojab, R. C. Powell, J. E. Greene, L. Hultman, and J.-E. Seindgren, Appl. Phys. Lett. **60**, 2491 (1992).
[10] P. Blaha, K. Schwarz, P. Sorantin, and S. B. Trickey, Comput. Phys. Commun. **59**, 399 (1990).
[11] K. Schwarz and P. Blaha, Lect. Notes Chem. **67**, 139 (1996).
[12] M. E. Sherwin and T. J. Drummond, J. Appl. Phys. **69**, 8423 (1991).
[13] P. E. Van Camp, V. E. Van Doren, and J. T Devreese, Phys. Rev. B **41**, 1598 (1990).
[14] A. F. Wright and J. S. Nelson, Phys. Rev. B **50**, 2159 (1994); **51**, 7866 (1995).
[15] K. Kim, W. R. L. Lambrecht, and B. Segall, Phys. Rev. B **53**, 16310 (1996).
[16] A. Tabata, R. Enderlein, J. R. Leite, S. W. da Silva, J. C. Galzerani, D. Schikora, M. Kloidt, and K. Lischka, J. Appl. Phys. **79**, 4137 (1996).
[17] R. Carles, N. Saint-Cricq, J. B. Renucci, M. A. Renucci, and A. Zwick, Phys. Rev. B **22**, 4804 (1980).
[18] G. Harbeke, O. Madelung, and U. Rössler, in *Physics of Group IV Elements and III-V Compounds*, Landolt-Börnstein, New Series, Group III, Vol. 17, edited by O. Madelung (Springer, Berlin, 1982).
[19] H.-J. Kwon, Y.-H. Lee, O. Miki, H. Yamano, and A. Yoshida, Appl. Phys. Lett. **69**, 937 (1996).
[20] T. Inushima, T. Yaguchi, A. Nagase, A. Iso, and T. Shiraishi, *Proceedings of the Sixth Conference on Silicon Carbide and Related Materials* (Institute of Physics, Bristol, 1996), Vol. 142, p. 971.

06 November 2025 18:57:40